SAND2017-11311C

Derivation of Six Degree of Freedom Shaker Inputs Using Sub-Structuring Techniques

Tyler F. Schoenherr
Analytical Structural Dynamics
Sandia National Laboratories[1]
P.O. Box 5800 - MS0346
Albuquerque, NM, 87185

Abstract

Multi-degree of freedom testing is growing in popularity and in practice. This is largely due to its inherent benefits in producing realistic stresses that the test article observes in its working environment and the efficiency of testing all axes at one time instead of individually. However, deriving and applying the "correct" inputs to a test has been a challenge. This paper explores a recently developed theory into deriving rigid body accelerations into a test article through sub-structuring techniques. The theory develops a transformation matrix separates the complete system dynamics into two substructures, the test article and next level assembly. The transformation does this by segregating the test article's fixed base modal coordinates and the next level assembly's free modal coordinates of the attached assembly. This transformation provides insight into the damage that the test article acquires from its excited fixed base shapes and how to properly excite the test article by observing the next level assembly's rigid body motion. The next level assembly's rigid body motion could be used as a direct input in a multi-degree of freedom test to excite the test article's fixed base shapes in the same way that it was in the working environment.

Keywords
Substructure, 6 DOF, multi-axis, component, testing

Introduction

Performing tests in a laboratory setting provides two large benefits to proving a product will perform as designed. These benefits are the cost and time that are saved by not performing field tests to prove design intent for a product. The ability to replicate failures experienced in the field quickly and accurately in the design phase saves a development program time and money. It also provides the opportunity to test the product's margin to determine the product's true factor of safety.

All of these benefits of laboratory testing is contingent on the laboratory test accurately producing the same strain and stress values that the product would experience in the field. The ability to replicate the field stress and strain values has proved over many years to be a very difficult task. Through the years this task has been separated into

[1]Sandia National Laboratories is managed by NTESS

two separate issues. The first is how to replicate the correct boundary conditions as to force the stress and strain fields to represent the field environment. The second issue is how to develop the forcing input to excite the structure to produce the same responses and consequentially the same stresses. Examples of complicated inputs could be multi-degree of freedom input at several mounting locations and acoustical loading. Some recent work has been done to address complicated forcing inputs [1] [3]. This paper will address how to form a set of six degree of freedom forcing inputs to a test article using a substructuring technique.

This paper demonstrates theory developed by Mayes [2] for a realistic complex system. It demonstrates how to take a model of the unit under test (UUT) along with its next level assembly and transform its coordinates to gain insight on stress that the UUT experiences and the rigid body inputs that are needed to cause those stresses.

To explore and demonstrate this theory, this paper uses a finite element model of the Box Assembly with Removable Component (BARC) hardware. The paper demonstrates the process of how a six degree of freedom (DOF) input to the removable component was derived to replicate the environment it experienced when it was attached to the box assembly. This paper discusses the results with respect to the process's shortcomings and successes and draws conclusions to their causes and effects.

Theory

The theory in this section was presented with respect to the BARC hardware referenced in the Introduction with a picture of the hardware shown in Figure 1. As in any substructuring problem, the different members must be identified and assigned names for clarity. Figure 1 provided a breakout of the different parts of the substructure and their corresponding names that will be used throughout this paper.

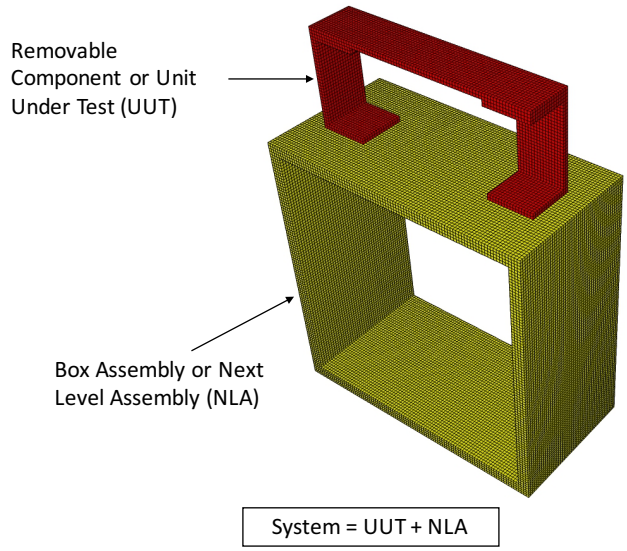

Figure 1: Pictorial of the BARC system

The derivation of this theory began by starting with the 2^{nd} order linear equations of motion of the next level assembly and the UUT assembled as a system,

$$\mathbf{M}_s\ddot{\bar{x}} + \mathbf{C}_s\dot{\bar{x}} + \mathbf{K}_\mathbf{s}\bar{x} = \bar{F}_s, \tag{1}$$

where $\mathbf{M}_s$ was the mass matrix, $\mathbf{C}_s$ the damping matrix, and $\mathbf{K}_s$ the stiffness matrix. The subscript s indicated the matrices were of the system. Modal substitution was used to estimate the physical response with modal degrees of freedom shown by

$$\boldsymbol{\phi}\bar{q} \approx \bar{x}, \tag{2}$$

where $\boldsymbol{\phi}$ was the mode shapes of the system and $\bar{q}$ was the generalized modal coordinates. The modal approximation shown in Eq 2 was substituted into Eq 1 and premultiplied by $\boldsymbol{\phi}^T$ to get

$$\boldsymbol{\phi}^T\mathbf{M}_s\boldsymbol{\phi}\ddot{\bar{q}} + \boldsymbol{\phi}^T\mathbf{C}_s\boldsymbol{\phi}\dot{\bar{q}} + \boldsymbol{\phi}^T\mathbf{K}_s\boldsymbol{\phi}\bar{q} = \boldsymbol{\phi}^T\bar{F}. \tag{3}$$

Scaling the mode shapes to be mass normalized allowed Eq 3 to be rewritten in terms of the system's modal parameters as

$$[-\omega^2\mathbf{I} + 2i\omega\omega_n\zeta_n + \omega_n^2]\bar{q} = \boldsymbol{\phi}^T\bar{F}, \tag{4}$$

where ω was the frequency in radians, ω_n was the natural frequency of the system with respect to each n mode, $\mathbf{I}$ was the identity matrix, and ζ_n was the modal damping factors with respect to each n mode. The damping factors and natural frequency vectors in Eq 4 were diagnolized square matrices of dimension $n \times n$. The system equations represented in Eq 4 were of a free system with only external forces acting on it.

It was at this point where a transformation matrix, T, was proposed to transform the modal degrees of freedom of the system to the fixed base degrees of freedom of the UUT, p, and the free modal degrees of freedom of the next level assembly, s, written as

$$\bar{q} \approx \mathbf{T}\begin{bmatrix}\bar{p}\\ \bar{s}\end{bmatrix}. \tag{5}$$

To formulate the transformation matrix, T, expressions had to be derived that related the modal coordinates of the UUT, p, and the next level assembly, s, to modal coordinates of the system, q.

A relationship between the s degrees of freedom and the q degrees of freedom was noted as

$$\boldsymbol{\phi}_b\bar{q} \approx \boldsymbol{\psi}\bar{s}, \tag{6}$$

where $\boldsymbol{\phi}_b$ was the mode shapes of the system at the degrees of freedom of the next level of assembly and $\boldsymbol{\psi}$ was the mode shapes of the next level assembly in a free condition. This relationship was a good approximation if the mode shapes of $\boldsymbol{\psi}$ span the space of $\boldsymbol{\phi}_b$. The relationship between q and s was completed by taking the pseudo inverse of $\boldsymbol{\phi}_b$ written as

$$\bar{q} \approx \boldsymbol{\phi}_b^+\boldsymbol{\psi}\bar{s}, \tag{7}$$

with the + symbol denoting a pseudo inverse.

Relating the fixed base degrees of freedom, p, to the free modal coordinates of the system, q, was done through component mode synthesis of analytically fixing the base [5]. This method developed constraint modes used to fix the system. The expression for this relationship was given as

$$\bar{q} \approx \mathbf{L}\boldsymbol{\Gamma}\bar{p}, \tag{8}$$

where the expression $\mathbf{L}\boldsymbol{\Gamma}$ was developed as the transformation of the fixed base modal coordinates to the free modal coordinates.

The transformation matrix, T, was then written as a concatenation of the relationships derived in Eq 7 and 8 as

$$\bar{q} \approx [\mathbf{L}\boldsymbol{\Gamma} \quad \boldsymbol{\phi}_b^+\boldsymbol{\psi}]\begin{bmatrix}\bar{p}\\ \bar{s}\end{bmatrix}. \tag{9}$$

The transformation given in Eq 9 was applied to the system's equations of motion in Eq 4 and the transform of T was premultiplied to get

$$T^T[-\omega^2\mathbf{I} + 2i\omega\omega_n\zeta_n + \omega_n^2]T\begin{bmatrix}\bar{p}\\ \bar{s}\end{bmatrix} = T^T\boldsymbol{\phi}^T\bar{F} \tag{10}$$

and can be rewritten as

$$\left(-\omega^2 \begin{bmatrix} \mathbf{I} & \mathbf{M}_{ps} \\ \mathbf{M}_{ps}^T & \mathbf{M}_{ss} \end{bmatrix} + 2i\omega \begin{bmatrix} \omega_{nfix} \cdot \zeta_{nfix} & \mathbf{C}_{ps} \\ \mathbf{C}_{ps}^T & \mathbf{C}_{ss} \end{bmatrix} + \begin{bmatrix} \omega_{nfix}^2 & \mathbf{K}_{ps} \\ \mathbf{K}_{ps}^T & \mathbf{K}_{ss} \end{bmatrix}\right) \begin{bmatrix} \bar{p} \\ \bar{s} \end{bmatrix} = T^T \boldsymbol{\phi}^T \bar{F} \tag{11}$$

The upper left hand partition in the transformed system matrices in Eq 11 corresponded to the fixed base modal parameters of the UUT and will be diagonal. The other partitioned sections of the newly formed **M**, **C**, and **K** matrices were fully populated and the off diagonals tied the two substructures together.

The transformation matrix, T, was derived to be square and not a reduction matrix. Because the transformation matrix was square and there was no reduction, the Eigen values and vectors after the transformation were unchanged.

There were a couple of characteristics of T that aided in interpreting its physical meaning. The transformation matrix was best thought of as a method of reorganizing the system's degrees of freedom to isolate the UUT from the next level assembly. The transformation matrix was interpreted as a linear combination of the fixed base modal coordinates of the UUT and free modal coordinates of the base to make up the free modal coordinates of the system.

Development of 6 DOF Specification

The purpose of using the theory presented in this paper was to take response data from a field test acting on the system and create a laboratory test to replicate the stresses of the UUT on a 6 DOF shaker table on a rigid fixture. The strategy used in this paper was to take the measured responses on the BARC system during a mechanical environment and transform them into p and s space utilizing the transforms defined in Eq 2 and 5 written as

$$\ddot{\bar{x}} = \boldsymbol{\phi}\mathbf{T} \begin{bmatrix} \bar{p} \\ \bar{s} \end{bmatrix} \tag{12}$$

and

$$[\boldsymbol{\phi}\mathbf{T}]^+ \ddot{\bar{x}} = \begin{bmatrix} \bar{p} \\ \bar{s} \end{bmatrix}. \tag{13}$$

As defined in the theory section, the s degrees of freedom were the free modes of the next level assembly or the box assembly in this case study. The s degrees of freedom could further be broken down to rigid (s_{rb}) and elastic modal coordinates (s_{el}). The s_{rb} motion was used directly as the input to the 6 DOF shaker table to control the rigid fixture to the same s_{rb} levels that were measured in the field environment. Because the inputs were derived directly from the time domain data, the phase between the rigid body modes was retained. The rigid body motion derived by this method would be identical to applying a rigid body modal filter to the next level assembly which is a common practice used for 6 DOF shaker inputs. However, the proposed method provided more insight into the test specification's effectiveness and accuracy.

Modal Analysis

Modal analysis of the BARC system and the removable component on a fixture was computed to gain insight on the structure and also to compute the necessary terms noted in the theory of this paper. The first four elastic mode shapes of the BARC system can be found in Figure 2 and the first three elastic modes of the removable component on the fixture can be found in Figure 3. All of the finite element analyses executed in this paper were computed by the SIERRA SD code package. [4]

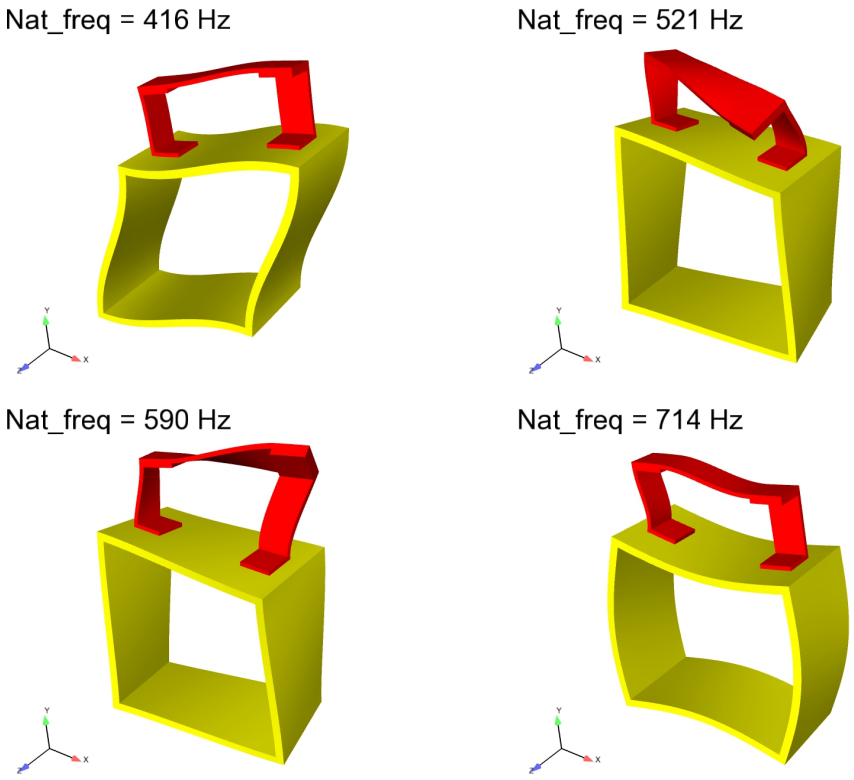

Figure 2: First four elastic mode shapes of the BARC system

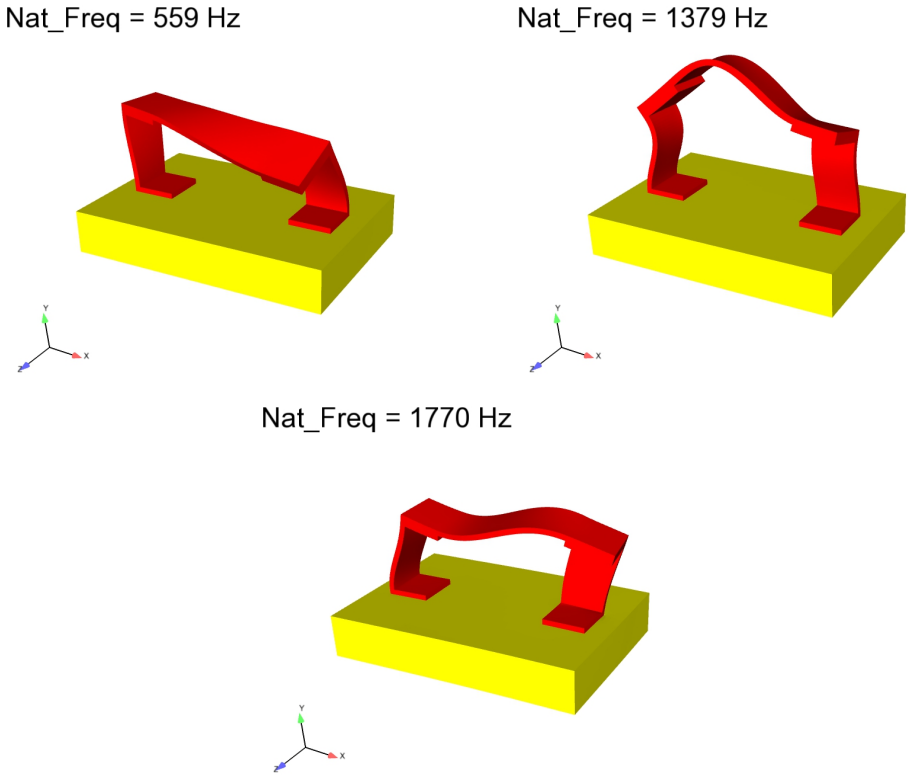

Figure 3: First three elastic mode shapes of the removable component on the fixture

Environments and Results

To determine if the theory and strategy laid out above were effective in reproducing the stresses experienced by the removable component in the environment test, two verification efforts were developed. The first verification effort was to input two sine waves individually into the system. The sine waves each had a frequency of 31 Hz to only excite the rigid body modes of the system. This was done so that the responses could be compared to hand calculations and verified for accuracy.

Figure 4 showed the two input locations on the box assembly and the response location on the removable component. All excitations and responses were input and measured in the y-direction per the coordinate system in Figure 4. These sine waves were applied and the responses at a subset of the total nodes were calculated. The responses were transformed using Eq 13 into p and s space. The first six values of s were segregated as the rigid body motion of the box assembly and that modal acceleration was enforced on the brick fixture in Figure 5.

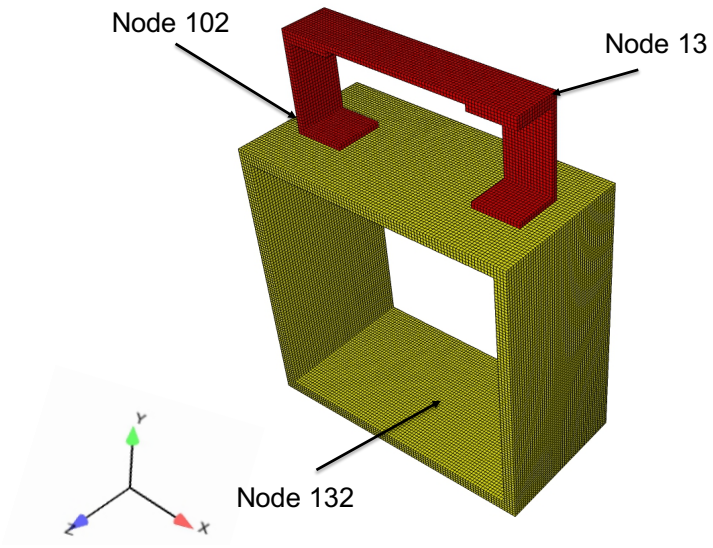

Figure 4: Input (nodes 132 & 102) and response location (node 13) for the rigid body tests on the BARC system

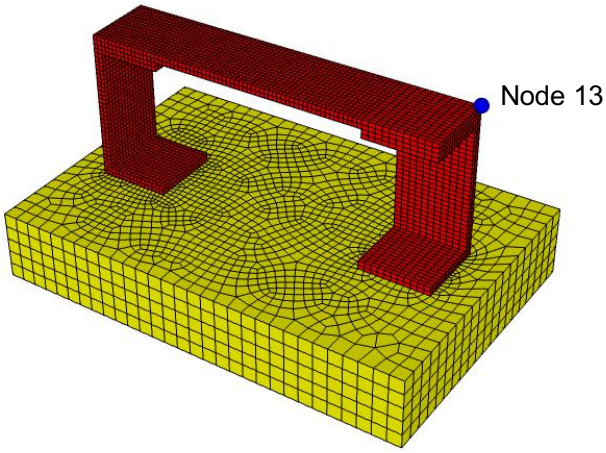

Figure 5: Pictorial of the removable component on a brick fixture

The response of Node 13 was calculated from the sine environment detailed above. The response of Node 13 was compared from the environment acting on the BARC system and on the fixture. This comparison was plotted in Figure 6. The replication of the acceleration of Node 13 in the two configurations showed that the theory could properly reproduce the environment for a rigid body input, translation and rotation.

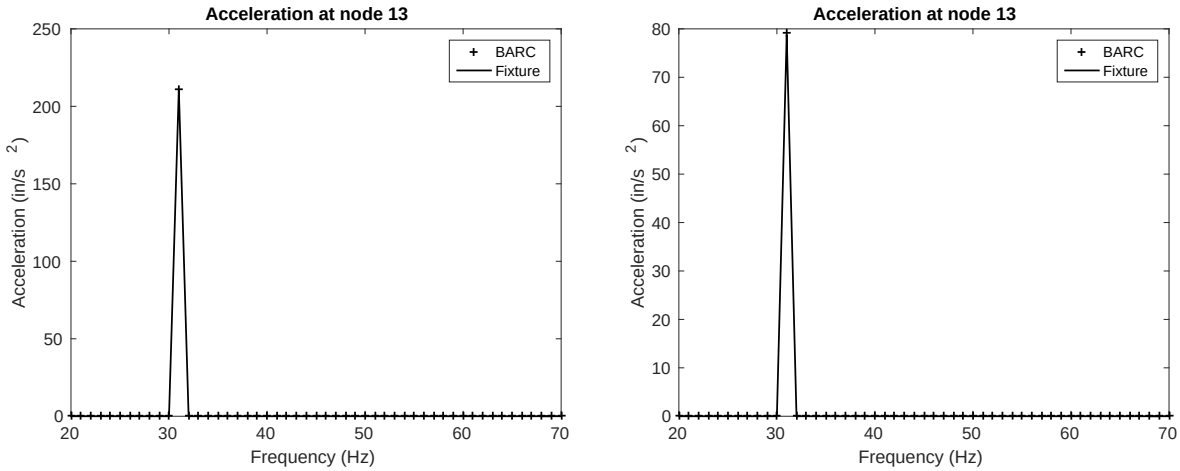

Figure 6: Comparison of response with a 31 Hz sine input at node 132 (right) and node 102 (left)

The second verification effort was to apply a flat random input that had energy content from 20 to 990 Hz at the location indicated by a blue dot in Figure 7, node 127. The load was input in the Z direction so that it would excite the modes of the system. From this environment, the s_{rb} motion was calculated as it had been previously and the acceleration of the fixture was forced to match the s_{rb} quantities calculated from the BARC environment.

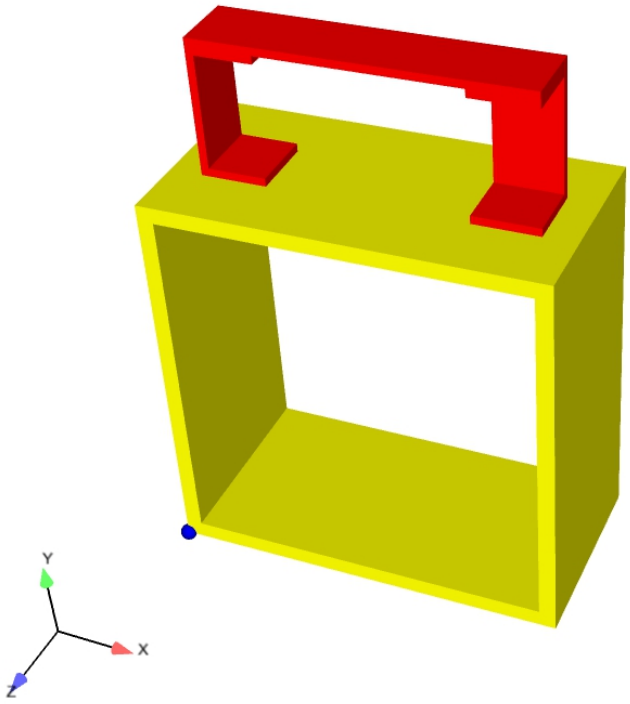

Figure 7: Excitation location for a random input in the Z direction at the blue dot (Node 127)

The response of Node 13 was compared between the random environment applied to the BARC system and the enforced acceleration that was applied to the test fixture. The comparison of acceleration was plotted in Figure 8. This comparison showed that there were several discrepancies between the two analyses. To examine the differences between the BARC and fixture analyses, the differences were examined at a mode by mode basis using the mode shapes in Figures 2 and 3. Historically, response of key nodes was a common method for determining the success of a test, however, the true parameter in determining a test's success was determined to be how the stresses that the test imparts on the UUT compares to the stresses in the field environment. Therefore, stresses per frequency line were calculated and compared.

The first and fourth modes of the BARC system were very poorly replicated by the fixture analysis and had orders of magnitude of error. Figure 9 showed that the stress profile and the levels were both incorrect for the first mode of the BARC system. Even though this case study showed that the stresses in the removable component were insignificant in both analyses, an excitation source on the BARC that better excited its first mode would have higher and potentially damaging stresses. The reason that the first and fourth modes were so poorly replicated was because the removable component was excited by the elastic mode of the box assembly, which the fixture could not replicate with rigid body motion.

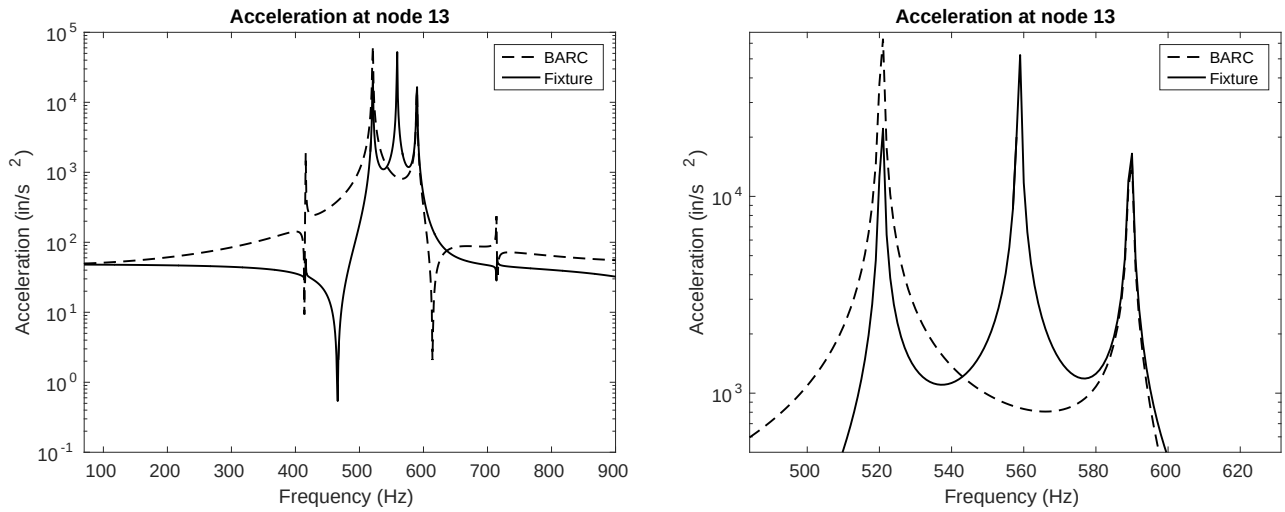

Figure 8: Response comparison of Node 13 on the BARC and fixture systems

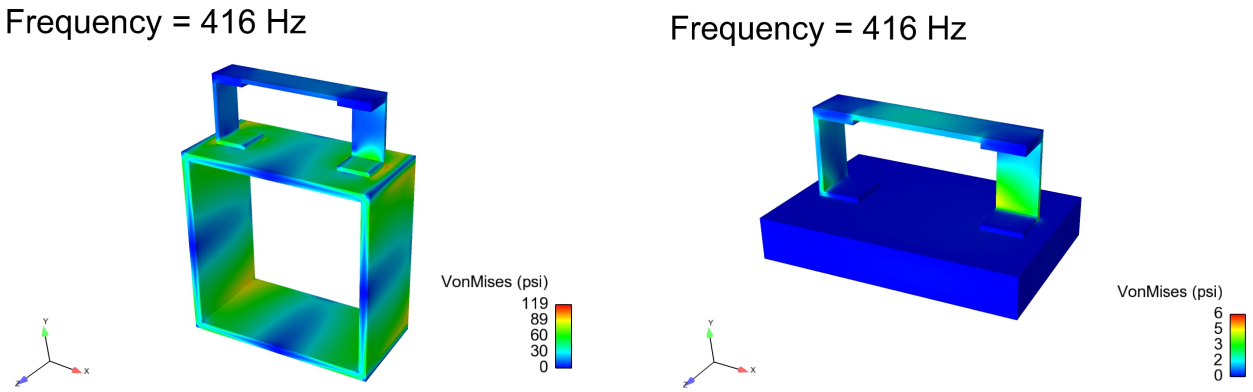

Figure 9: Excitation location for a random input in the Z direction at the blue dot (Node 127)

The second and third mode shapes of the BARC system and first mode of the fixture system all appeared to have similar shapes for the removable component. The shape resembled the first fixed base mode of the removable component. The analyses of the BARC system and the fixture system produced stress fields that were shown in Figure 10. Observation of these stress plots showed that the stress profile of the removable component was very similar between the two modes and the two systems. However, the fixture system was an under-test of 32% for the second shape and was an over-test of 2% for the third shape. Figure 8 also showed a resonance that was not in the BARC system that was excited in the fixture system. This was the first mode of the fixture system at 560 Hz and was a large over-test. Because the rigid body motion of the base was the control parameter, there was no feedback parameter to filter the test configuration's first natural frequency.

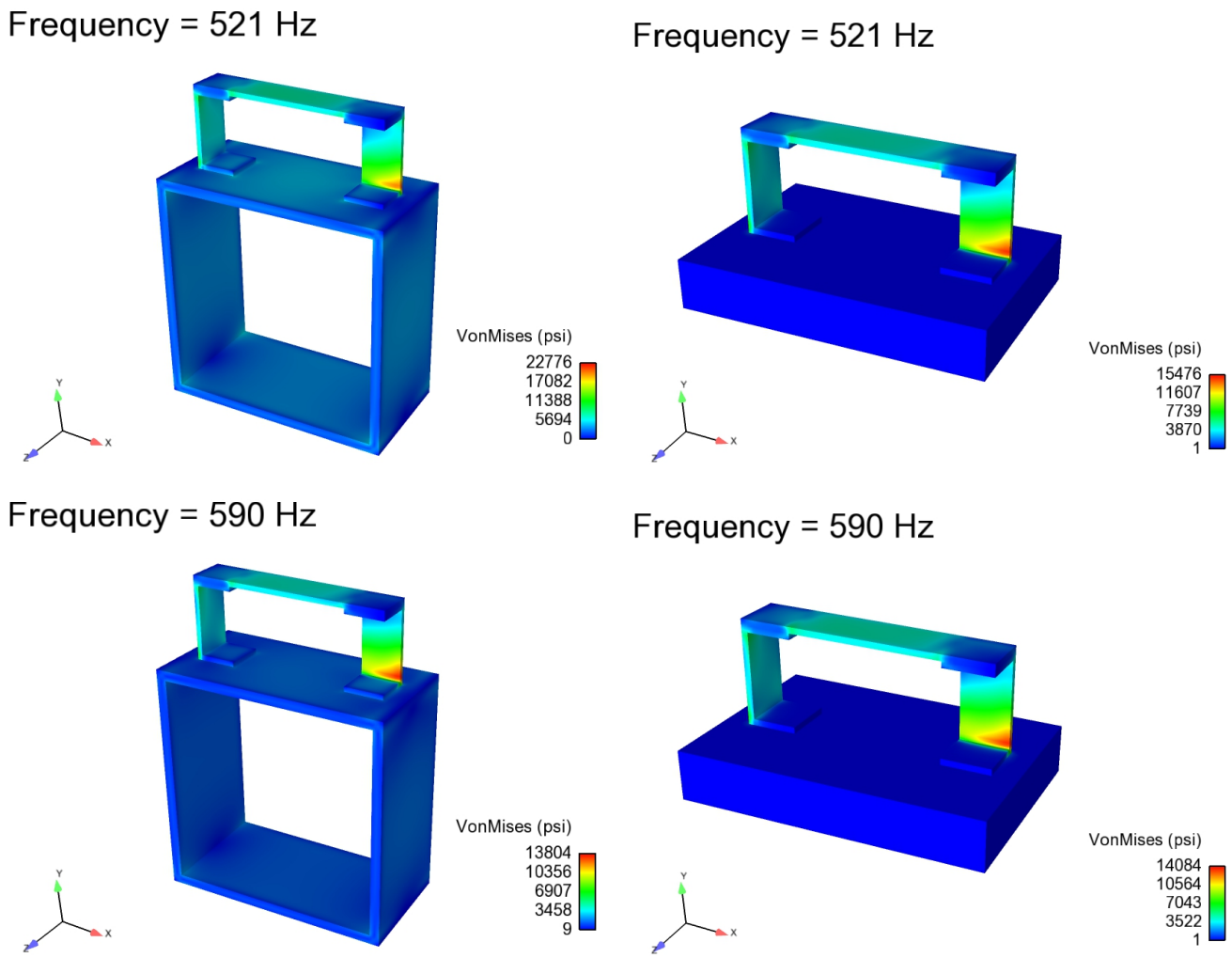

Figure 10: Von Mises stress from the flat random environment at node 127 (left) and test environment (right)

This case study showed that the elasticity of the next level of assembly interacted with the unit under test. It was proven that this interaction was a factor in how successful the fixture system can replicate the stresses of the BARC system. Through the development of this case study, it was decided to qualitatively compare the s_{rb} degrees of freedom to the s_{el} degrees of freedom of both the BARC and fixture systems. The result of this comparison was plotted in Figure 11.

Upon examination of these plots, it was determined that this qualitative comparison was an indicator on how influential the elastic motion of the next level assembly was on the motion and stress of the unit under test. This conclusion was reached because the s_{el} degrees of freedom were the same or higher than the s_{rb} degrees of freedom for the BARC assembly and the box assembly was proven to have significant interaction with the removable component. Conversely, the fixture had little influence on the removable component as the s_{rb} degrees of freedom were about two orders of magnitude higher than the s_{el} degrees of freedom.

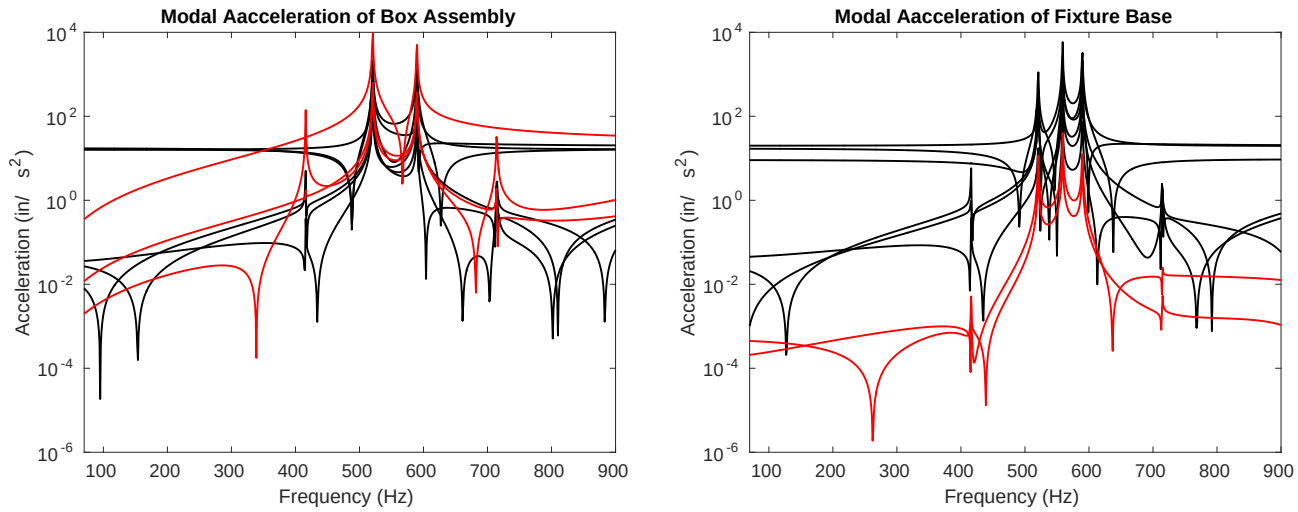

Figure 11: S rigid body degrees of freedom (black) and S elastic degrees of freedom (red) for the BARC and fixture system

Conclusion

Dynamic substructure theory previously developed was applied to a real life structure with the intent of creating a six degree of freedom shaker test. This application was tested and was shown to have large similarities to calculating the input with a rigid body modal filter. Although the underlying physics were the same, more insight was produced through the substructuring method as the degrees of freedom of the unit under test and the next level assembly were separated and observable.

The effectiveness of the theory was limited as the interaction or impedance of the next level assembly had an effect on the stresses of the unit under test. The fixture was rigid in the frequency range where the box assembly had modes. These modes were only important if they caused any stresses on the removable component.

Comparing the s_{rb} degrees of freedom coordinates to the s_{el} degrees of freedom indicated how well a rigid fixture could replicate the motion of the next level assembly. This comparison could be used as a parameter or check to determine if a six degree of freedom shaker table would be an appropriate means of replicating a mechanical environment.

References

[1] P. M. Daborn, C. Roberts, D. J. Ewins, and P. R. Ind. *Next-Generation Random Vibration Tests*, pages 397–410. Springer International Publishing, Cham, 2014.

[2] Randall L. Mayes. *A Modal Craig-Bampton Substructure for Experiments, Analysis, Control and Specifications*, pages 93–98. Springer International Publishing, Cham, 2015.

[3] Jesus M. Reyes and Peter Avitabile. Adjustment of vibration response to account for fixture-test article dynamic coupling effects. In *Proceedings of the 35th IMAC*, Feburary 2017.

[4] Sierra Structural Dynamics Development Team. Sierra structural dynamics - user's notes. Technical Report SAND2017-3553, Sandia National Laboratories, April 2017.

[5] Brandon R. Zwink, Randall L. Mayes, David W. Kelton, Jack D. Heister, Patrick S. Hunter, and Anthony J. Gomez. *Converting a Slip Table Random Vibration Test to a Fixed Base Modal Analysis*, pages 341–357. Springer New York, New York, NY, 2012.